

# Optimization of Groundwater Pumping and River-Aquifer Exchanges for Management of Water Resources

Mayank Bajpai<sup>1</sup>, Shishir Gaur<sup>1</sup>, Anurag Ohri<sup>1</sup>, Shreyansh Mishra<sup>1</sup>, Hervé Piégay<sup>2</sup>, and Didier Graillet<sup>3</sup>

<sup>1</sup>Indian Institute of Technology BHU Varanasi

<sup>2</sup>CNRS

<sup>3</sup>Ecole des Mines de Saint-Etienne

September 24, 2021

## Abstract

Groundwater pumping influences the rate of River-Aquifer (R-A) exchanges and alters the water budget of the aquifer. Therefore, fulfilling the total water demand of the area, with an optimal pumping rate of wells and optimal R-A exchanges rate, is important for the sustainable management of water resources and aquatic ecosystems. Meanwhile, comparison of the output of different simulation-optimization techniques, which is used for the solution of water resource management problems, is a very challenging task where different Pareto fronts are compared to identify the best results. In the present work, mathematical models were developed to simulate the R-A exchanges for the lower part of the River Ain, France. The developed models were coupled with optimization models in MATLAB environment and were executed to solve the multi-objective optimization problem based on the maximization of pumping rates of wells and maximization of groundwater input into the river Ain through R-A exchanges. The Pareto front developed by different simulation-optimization models was compared and analyzed. The Pareto fronts were juxtaposed based on the convergence, total diversity, and uniformity with the help of different performance metrics like hypervolume, generational distance, inverted generational distance, etc. The impact of different groundwater models based on domain size and boundary conditions was also examined. Results show the dominance of MOPSO over other optimization algorithms and concluded that the maximization of pumping rates significantly changes after considering the R-A exchanges-based objective function. It is observed that the model domain also alters the output of simulation-optimization, therefore the model domain and corresponding boundary conditions should be selected carefully for the field application of management models. ANN models were also developed to deal with the computationally expensive simulation model by reducing the processing time and were found efficient. Keywords: Simulation-Optimization, Multi-Objective optimization, Artificial Neural Network, River-Aquifer exchanges.

## 1. Introduction:

River-aquifer (R-A) exchange influences both quantity and quality aspects of groundwater and river water systems significantly. Consequently, proper and effective quantification and representation of river-aquifer exchange are very important for the management of water resources and aquatic ecosystems. Climate and groundwater pumping for irrigation has caused rapid groundwater depletion in India (Dangar et al., 2021). Several works have been carried out about the identification and the quantification of groundwater and surface water interactions i.e. R-A exchanges (Constanzt, 1998; Sophocleous, 2002; Becker et al., 2004; Anderson, 2005; Kalbus et al., 2006; Keery et al., 2007; Lowry et al., 2007; Yang et al., 2017). Some studies on R-A exchanges also demonstrate the effect of it on river temperature (Westhoff et al., 2007; Burkholder et al., 2008; Hebert et al., 2011) along with the emphasis on exchanges in hyporheic zone (Burkholder et al., 2008).

Simulation-optimization (S-O) techniques are often used in identifying the optimal management practices of groundwater for the selected region. Many challenges are associated with this S-O technique like the selection for proper simulation or optimization algorithm and comparison of the results of various techniques used. In the multi-objective optimization problems, comparison of results becomes more significant as Pareto fronts generated in this approach can have some similarities with some diversity. Jha et al. (2020) statistically evaluated the relationship between groundwater pumping rates and groundwater levels during pre-monsoon and post-monsoon seasons using a numerical groundwater-flow simulation model. The simulation-optimization (S-O) model used linear programming (LP) optimization to handle groundwater hydraulic optimization management problems after convolution techniques were employed to integrate the simulation model with an optimization method. Kamali Asghar (2017) used a mathematical simulation optimization programming model to handle the issue of aquifer management, relying on the stability of water quality and quantity. The simulation-optimization models and the construction of the sustainability index for determining the best point of the Pareto front were used in the study's modeling. Abd-Elmaboud et al. (2021) introduced a new model that connects geomorphological and hydrogeological data with recharge rates. The MFUSG-PSO model with an indirect simulation-optimization technique for the inversion of the groundwater flow problem was used to calibrate the recharge rates. The second phase involved training a CFNN model to connect the calibrated recharge rates with freely available geomorphological and hydrogeological data to construct interrelationships. For the best possible conservation of water resources, Conant et al. (2019) suggested that it is critical to understand and quantify exchange activities between rivers and groundwater. The exchange between rivers and groundwater is significant in a variety of current concerns, including providing drinking water, characterizing and managing environmental flow regimes, preserving or restoring riverine ecosystem health and functioning, and alleviating toxins. For reaches in plains with flow monitoring data. Li et al. (2020) introduced a cumulative exchange fluxes method based on surface water balance to study GW-SW interactions. The dynamic change processes of GW-SW interactions can be qualitatively and quantitatively judged through a curve of cumulative exchange fluxes by this method. The hyporheic zone, which is usually regarded as a biogeochemical hotspot, is where surface-groundwater interactions are most frequent and according to McClain et al. (2003), these hotspots are the key to manage water resources effectively.

Calandra et al. (2014) proposed an approach to make full use of the simulation algorithms developed by Bayesian Optimization to analyze the quality of Pareto fronts, unlike the existing algorithms which only returned the Pareto solution sets without considering the qualitative assessment. The approach was able to delineate the actual Pareto fronts better in presence of noise and at the same time can also perform sensitivity analysis of the parameters concerning the quality of model output. Lobato et al. (2016) have presented a Bayesian method called PESMO to identify Pareto solution set to Multi-Objective optimization problems. The evaluation points were chosen as such to minimize the entropy of the Pareto set. When compared with existing techniques, PESMO was found to produce better results with a smaller count of evaluations, while the decoupled estimation led to an improved performance particularly when the existing techniques lose efficiency with an increase in objectives. Emmerich et al. (2018) have also discussed the fundamentals and evolutions in the field of Multi-objective optimization. The topics covered in their article include- order-theoretical foundations, scalarization approaches, and optimality conditions. In context to the evolutionary methods, three state-of-the-art techniques were discussed namely NSGA-II, SMS-EMOA, and MOEA/D. NSGA-II representing the Pareto-based approach, SMS-EMOA exemplifies the Indicator-based approach while MOEA/D is an example of a decomposition-based approach. The choice of the correct technique depends on the number of objectives, count of solution sets, desired distribution of the solutions along with the location and shape of the Pareto front. Belakaria et al. (2019) have addressed the optimization of the Multi-Object (MO) black box to determine true solutions of Pareto-set by reducing the count of function evaluations. The study proposed a new algorithm called Max-value Entropy Search for Multi-objective Optimization (MESMO) to ascertain an optimized design that efficiently trades off among performance, power requirement, and area overhead. Their approach used the output matrix entropy function to efficiently select the input parameters, to obtain highly accurate Pareto-set solutions. The algorithm was found to be constantly outperforming the existing state-of-the-art algorithms in computing Pareto set solutions.

Binois et al. (2014) have taken into account Kriging metamodel for estimating the Pareto front and also to quantify bias associated with the solution set at any phase of the multi-objective optimization. The approach taken by them assumed the original dataset to be having Gaussian distribution. The concept of random set theory has been used to compute Vorob'ev deviation to capture the variability of the dataset with non-dominated points. This method applied on several numerical problems yielded satisfactory output in accurately determining of Pareto front. Horn et al. (2016) proposed a model based on Random Forests for model-based multi-objective optimization to determine the Pareto front for mixed hierarchical configuration problems. A two-phase parameter experiment was carried out. The results of the single model experiment were quite promising, however, the solution derived through a multi-model approach could be improved further. Especially, the bias estimation associated with the Random Forest model needed to be resolved.

Cao et al. (2017) have tried to quantify the bias of the estimated solution of multi-objective problems using two versions of the normalized hypervolume. A case study was carried out in a chemical process with three sets of solutions, each having a different optimization goal. Results showed that the normalized hypervolume showed great accordance to the ideal situations while taking into account the degree of the trade-offs between the possibilities considered to compute the front. Bassi et al. (2018) have considered a new approach to evaluate statistical parameters for a set of objects equivalent to surfaces and arcs. Their approach is based on the identification of the most representative member of a family tree and was found useful to address the uncertainties associated with Pareto fronts. The Pareto front was ascertained by minimizing the hypervolume between the front and the reference points. The algorithm was tested on a complex 5 bar truss structure with satisfactory outputs being obtained. Avent et al. (2019) proposed a new approach called DPARETO, to determine the trade-off among various differentially cloistered algorithms. Bayesian Optimization (BO) was used to concurrently optimize both privacy and utility parameters of a Pareto front. Moreover, they also established the effectiveness of BO in creating visualization interfaces helpful in decision making. Bionis et al. (2019) have designed a GPareto library for R which enables the optimization of multi-objective algorithms for functions associated with a black box. Moreover, the package also contained several algorithms for the accurate assessment of the associated bias. The study also proposed several infill criteria in minimizing the bias associated with several optimization models such as efficient global optimization technique.

Marjit R. (2009) has made a noble attempt to increase the efficiency of the Building performance simulation (BPS) tool by combining it with a robust multi-objective optimization algorithm. The thesis aimed at developing a multi-objective algorithm with a meta-model to optimize the simulation of a Pareto front. Asadzadeh et al. (2014) on the other hand, have developed a new technique called Convex Hull Contribution (CHC) to address multi-objective (MO) optimization functions associated with Pareto fronts. They demonstrated the effectiveness of CHC in enhancing the accuracy of Pareto archived multi dimensioned search while addressing the multi-objective problems. Audet et al. (2018) have presented a review of the algorithms devised so far to address the multi-objective-based optimization in the determination of Pareto fronts. An assessment of a large number of performance indicators was carried through various algorithms. Total 57 performance indicators were grouped into four categories by their properties, viz. cardinality, convergence, distribution, and spread. Hollermann et al. (2019) have proposed a new flexible method to automatically identify one optimum design for multi-objective decision-making. Their approach addresses both economic and environmental aspects to identify a viable design. The bias associated with the parameters while predicting a future event could be handled easily by developing an extension of this algorithm.

Present work was carried out to address the challenging issue of R-A exchanges which can be analyzed through numerical models. The output of the numerical models depends on the model domain considered, different hydrogeological parameters used and boundary conditions applied. Considering the R-A exchanges in groundwater resource management problems can help in finding out more efficient and river health inclusive management practices through simulation-optimization models. Meanwhile, selection of the optimization algorithm, model domain demarcation and the comparison of optimum results to provide a physically meaningful management strategy is still a bottleneck in the groundwater management problems. Therefore, different model domain demarcations for the same river system were considered for the development of the groundwater model, and their impact on R-A exchanges was analyzed. In addition, different

optimization techniques were also used and their outputs i.e. Pareto fronts were compared. Finally, this set of optimal results were interpreted in terms of groundwater management.

## 2. Study Area:

The Ain River has an oceanic hydrologic regime and drains a basin of about 3630 km<sup>2</sup>. It is located in the southern Jura Mountains, France. The length of the Ain River is about 200 km and it is the right bank tributary of the Rhône River. The lower part of the Ain River, which is located between the Allement dam and the confluence with the Rhône River, was taken for the study purpose. Figure 1 shows the location of the lower Ain river area. Along this section, the average channel width is about 60 m and the slope is about 1.3%. The mean annual discharge of the river, between 1959 to 2019, was evaluated as 120 m<sup>3</sup>/s at the measuring station of Chazey-sur-Ain. Most floods occur between October and March (probability of occurring flood discharge of 1200 m<sup>3</sup>/s, once in 10 years, at Chazey-sur-Ain) and summer is characterized by low flow conditions. Further detail about the study area is provided in the groundwater model section.

## 3. Methodology

Two major objectives were addressed in this study. The first objective was to identify the maximum pumping rates of the wells by considering the R-A exchanges component. This also includes examining the impact of different types of model domains on the output of R-A exchanges and to find the best model domain and boundary conditions. Whereas the second objective was to compare the Pareto front developed by different coupled simulation-optimization models. Different groundwater model domains were taken by using the different boundary conditions and the impact of each domain on R-A exchanges and correspondingly the water budgeting of the aquifer was examined. Figure 2 shows the flow chart of the methodology. Total four optimization techniques were compared i.e. Multi-objective Genetic Algorithm (MoGA), Multi-objective Particle Swarm Optimization (MOPSO), Pareto Search (PS), and Multi-Objective Evolutionary Algorithm based on Decomposition (MOEA/D). To deal with a large number of wells, the wells in the domain were grouped based on the municipal zones and distance of the wells from the river. If any well in the municipal zone had a distance from the river less than a threshold of 1 km, then it was classified as a new well zone.

In the objective functions, maximum pumping rates in the well zones and maximum groundwater inflow into the river were considered. Conceptual models in GMS-MODFLOW (Groundwater Modelling System, Aquaveo) were developed to simulate the river-aquifer exchanges for the lower part of the River Ain, France and these were coupled with optimization models available in the MATLAB platform. To implement the coupling between the two systems, MATLAB scripts were developed which carried out the following tasks, (i) run the optimization model with Modflow as cost function, (ii) read and write the decision variables from the '.h5' input file for Modflow, (iii) run the simulation model, extract and post-process the output of simulation model to calculate a cost for optimization model.

Additionally, the sets of optimized costs (Pareto fronts) were compared using various criteria (convergence, diversity, and uniformity) and metrics (hypervolume, spread, and IGD). Decision variables corresponding to these Pareto fronts were also compared in terms of spatial and quantitative distribution in different model domains.

### 3.1 Groundwater Model Development :

The groundwater flow modeling was performed using MODFLOW. GMS 10.4 based on conceptual model approach was adopted to create different geospatial data-based input layers for defining the surface recharge, boundary conditions, discharge wells, observation wells, and hydraulic conductivity of the area and to build the groundwater model. The piezometric surface of groundwater was created using hydrograph data of 280 wells in the study area.

The topography, top, and bottom of the study area, was found in the range of 240 m to 550 m where SRTM data was used to get the surface elevation of the area. The bottom surface was prepared with the help of well log data obtained by BRGM. The two-layered model was developed for the underlying sediments where each layer was assumed to be horizontal, homogeneous, and isotropic. The mean thickness of the layer was taken

as 25 m. The initial values of hydraulic conductivity were taken from 0.0018 m/s for the older sediment and 0.003 m/s for the younger sediment. The horizontal hydraulic conductivity was estimated from the pumping well test data and the literature data obtained by BRGM. Thus, the obtained data have been used as initial distributions that were subsequently modified during calibration of the numerical model to achieve the best fit between the simulated and the observed data. Specific yield (Ss) values for the alluvial deposits were found in the range from 1 to 17%.

*Boundary Conditions:* The model was developed by defining two types of external model boundaries i.e. constant head and constant flow boundaries. Figure-3 shows the different types of domains that were considered to perform the groundwater modeling. The figure shows that in the Domain-1, eastern & western sides of the model domain were defined based on watershed divide line i.e. no-flow boundary respectively, whereas in Domain-2 alluvium plain of the Ain river were considered and the eastern & western side of the model domain was defined based on constant flow boundaries. The constant flow values were referred to from the published report of BRGM (Ref.). Whereas, the model Domain-3 was chosen the same as Domain-1 with one modification in the lower eastern part. The Rhone river was introduced in the model domain through the constant head boundary. This modification helped to find the impact of incorporating the Rhone river in the modeling area.

*Piezometer and River water level data:* In this study, a total of 15 piezometers were available, where a few piezometers had data for the period of 2008 to 2010 and the remaining piezometers covered the data from 2002 to 2015. The data thus collected, showed that the piezometer doesn't show very high fluctuation in values. This variation ranged from 3.7m to 1.2m, which showed that the groundwater table, and correspondingly groundwater scenario, is very stable in the region. Further, the river water level data, which was measured at 5 locations of the study area, was obtained from Banque Hydro France. The data from 2002 to 2015 was also examined to understand the trend of data. This analysis showed a fluctuation range of 2.54 m at Chezy and 1.67m at point de'Ain on the river Ain. Data of other tributaries such as Albarine also showed a maximum fluctuation of 1.36m.

*Recharge & Evapotranspiration:* Rainfall was considered as the source of groundwater recharge. Rainfall data from the Météo France database was used to calculate the recharge input values and applied uniformly over the polygons constructed in the model domain. The different recharge polygons were developed based on a land-use map created from satellite imageries (Figure 6). Six categories were taken for classification purposes such as water body, agriculture, fallow land, built-up, forest/vegetation, sand. Supervised classification was performed to create the land-use map where the fusion of Satellite imageries of Sentinel 1 and Landsat 8 was used. In Sentinel-1 bands, VV and VH were used whereas in Landsat 8 bands 1 to 7 were used for classification purposes. Random Forest model was used as classifier and training accuracy, test accuracy, and kappa coefficient were 99.98% 98.45%, and 97.77% respectively. The initial value of recharge was taken as 10%, 50%, 50%, 80%, and 60% for built-up, agriculture, vegetation, sand, and fellow land of total precipitation i.e. 1650 mm/year. Estimated evapotranspiration was taken as 638 mm/year with an extinction depth of 2 m. The potential evapotranspiration was considered uniformly distributed over the study area. For the future forecast, 10 years' monthly average of rainfall were taken and corresponding recharge values were used.

*Water Demand and Supply:* Water consumption in the study area is mainly done by agriculture, the rest is used for domestic purposes and some for industrial usage. The discharge details about the wells were computed on the basis of agricultural and domestic demands of the area. The field survey was carried out to collect the information of water demand as per the cropping pattern and domestic water consumption. The total agriculture water demand was identified through the classification of satellite imagery data for three seasons. The groundwater abstraction varies seasonally as well as yearly due to variable demands for irrigation. The quantitative data, available from 2002, are obtained from three sources - the Rhône-Méditerranée-Corse Water Agency (AERMC), the Directorate Department of Agriculture and Forestry (DDAF), and the Association Syndicale of Ain Irrigation (ASIA). The groundwater abstraction is divided into three uses (Table 1). Thus, the total catchments identified are 372, representing a total annual volume of 40,130,104 m<sup>3</sup>. which varies up to 27 Mm<sup>3</sup> in some conditions. The total water requirement computed by this method is found to

be 106.78 mcm, which is 5% more than the value available by administrative authority i.e., 101.43 mcm.

**Calibration and Validation:** A regional groundwater flow model was constructed and calibrated to the transient-state condition with a stress period of four months. In the calibration of the model, the value of recharge and boundary inflow was taken. Calibration of the model was performed based on computed and observed values of groundwater head at 20 evenly distributed points in the study area. Based on the availability of data, the model was calibrated from 2008 to 2010 based on all piezometers and further from 2010 to 2012 on the basis of remaining wells. The further model was validated based on data from 2012 to 2015. In the calibration processes, the groundwater head values which were computed by the model and observed at the observation wells were analyzed at 95% confidence level (Figure 4) at four different locations. The mean square error was computed for the calibration process. The differences between observed and computed values were found less in the middle part of the valley whereas on the boundary of the model domain they were not found within the range of the 95% confidence level due to inaccuracy for defining the head flux boundaries. Therefore, head flux boundary values were modified within the range of 10%, and the effect on the error was observed. Initially, the constant flow boundary was calibrated in the study state condition to incorporate the groundwater in-flow from the adjacent aquifer. The recharge rate was calibrated with the help of PEST (a popular parameter estimation program) in the MODFLOW package. Final outputs of the model were obtained as water table contour maps and directions of groundwater movement together with mass water balances for the model domain, and river-aquifer exchanges. Further, river-aquifer exchanges were calculated with the help of a calibrated model.

### 3.2. Optimization Problem

The objective of the optimization model is to maximize the water withdrawal rate from the aquifer (Total discharge,  $Q$ ) and water gain of the river from the aquifer (Leakage out,  $L$ ) while having the least drawdown at the wells in the domain. The leakage out represents the rate of discharge of water from the aquifer to the river. The pumping rate is assumed constant over well zones and specified time steps. The water withdrawal rate from the well zones, leakage rate out of the aquifer into the river, and drawdown at the wells, of the last time step, are considered for optimization. The domain contains different zones of the wells, based on the distance from the river and municipal zone data. To achieve the objective, the discharge in these zones are adjusted by the following optimization algorithm:

$$\text{Maximise } \left\{ \begin{array}{l} \sum_{i \in R} L_i - P \\ \sum_{i=1}^{n_z} N_i * Q_i - P \end{array} \right.$$

$$(Q_i)_{lb} \leq Q_i \leq (Q_i)_{ub}$$

where,  $L_i$  = rate of leakage out of the aquifer to the river;  $Q_i$  = rate of discharge of  $i^{\text{th}}$  well zone;  $R$  = set of the river grid cells with leakage out;  $n_z$  = total number of well zones;  $N_i$  = number of wells in the  $i^{\text{th}}$  zone;  $P$  = penalty imposed due to drawdown constraint violation;  $(Q_i)_{lb}$  = lower bound of the discharge for the  $i^{\text{th}}$  well zone;  $(Q_i)_{ub}$  = upper bound of the discharge for the  $i^{\text{th}}$  well zone.

$$\text{dist} = \sqrt{\sum_{i \in W} (d_i - d_{\text{threshold}})^2}$$

$$P = C_{\text{model}} * d_{\text{dist}}$$

Where,  $d_i$  = drawdown at  $i^{\text{th}}$  well;  $W$  = set of wells;  $d_{\text{threshold}}$  = threshold value of drawdown, taken as 2 m;  $d_{\text{dist}}$  = distance-based metric for drawdown;  $C_{\text{model}}$  = constant to amplify the penalty. The value of  $C_{\text{model}}$  is calculated such that the penalty is of the same order as that of the cost. Both the cost has values of the order  $10^5$  and from the multiple (500) random model evaluations, an expected value of  $d_{\text{dist}}$  is obtained. Consequently, the value of the  $C_{\text{model}}$  is obtained as  $10^5 / E(d_{\text{dist}})$ .

### 3.3. Optimization Techniques:

Four techniques viz. MoGA, MOPSO, PS, and MOEA/D were compared on three groundwater model domain sizes. MATLAB provides inbuilt functions for the implementation of MoGA and PS. The following subsections discuss the details of the optimization algorithms.

**3.3.1 Multi-objective Genetic Algorithm:** In MATLAB, ‘gamultiobj’ is the function used for the Multi-objective GA. This function uses a controlled and elitist genetic algorithm (The MathWork Inc.), which is a variant of NSGA-II (D. Kalyanmoy, 2001). This algorithm increases the diversity by favoring a variety of individuals even if they have a lower fitness value. After the initialization, generic operations (crossover, mutation, and selection) are iteratively performed. Consequently, crossover fraction, mutation rate, number of generations, and population size are major parameters affecting the performance of the algorithm. For the ANN model, these parameters were set to 0.85, 0.015, 2000, and 200 respectively, and for the simulation model, these were set as 0.85, 0.015, 150, and 25 respectively.

**3.3.2 Multi-objective Particle Swarm Optimization:** This heuristic algorithm is inspired by the movement of a bird flock. Each bird or particle has a position and local velocity in the feasible solution domain. The exploration of the domain by these particles is governed by both local and global velocity, which are computed based on the personal best and the global best solution obtained in the domain. In Coello et. al. (2004), the most widely used implementation of MOPSO introduced a mutation operator that enriches the exploration capability of the algorithm. Víctor Martínez-Cagigal (2020) provides a MATLAB implementation of Coello et. al. (2004), which is used in this work. The  $c_1$  and  $c_2$  were set to 2 for both ANN and simulation models. Maximum iterations and number of particles, for the ANN model, were set to 1000 and 100 respectively. For the simulation model, these were 150 and 25.

**3.3.3 Pareto Search:** The Pareto search algorithm by MATLAB, finds the non-dominated solution by the use of Pareto search in a set of points (archives and iterates). The algorithm uses the poll to find better solutions and if no better solution is available, then in the next iteration half multiply the mesh size. Theoretically, the algorithm converges to points near the true Pareto front (The MathWork Inc.). In MATLAB, *paretosearch* function is used for its implementation. Also, it takes fewer function evaluations than *gamultiobj* and it performs better or equal, in comparison to NSGA-II if there are no non-linear constraints (The MathWork Inc.). No parameter tuning is required for the Pareto search algorithm, though stopping criteria based upon tolerance and time can be adjusted.

**3.3.4 Multi-objective Evolutionary Algorithm Based on Decomposition:** MOEA/D solves a multi-objective by decomposing it into multiple scalar sub-problems and solving them simultaneously. The solution of these sub-problems is evaluated based on its neighboring sub-problems, which makes its computational cost lower in each generation in comparison to NSGA-II (Zhang et.al. 2007). Polynomial mutation (order  $n$ ) is used as the mutation function. Several sub-problems, maximum iterations, percentage of the neighborhood, and mutation rate are the major parameters for MOEA/D. For the final ANN model, these parameters were set to 1500, 100, 40%, and  $1/n$  respectively. For the simulation model, these were set to 100, 20, 40%, and  $1/n$  respectively.

The use of these algorithms is computationally expensive with the groundwater simulation models, which require few seconds for a single run and require days to complete the single solution. Therefore, an ANN model is also developed to speed up the evaluation of cost function. The efficiency ANN-Optimization model is majored with the performance of the actual simulation-optimization algorithm by performing a feasible number of simulation runs. The ANN model was trained with a dataset generated by simulation models itself. The parameters of optimization algorithms are set to improve the solution set at the cost of increasing the number of simulations which is accommodated by the ANN model.

### 3.4. ANN-Optimization model

ANN is a widely used technique to map non-linear and black box functions for fast evaluations. Feed Forward Neural Network (FFNN) is the most commonly used ANN. It consists of multiple parallel layers of memory

units (neurons). Each layer of neuron is fully connected with its adjacent layer and the strength of the connection is defined as its weight. The backpropagation technique is used to find these weights such that error between the actual and predicted values, is minimized.

For this work, nearly  $10^4$  random data points, with zone-wise discharge as input and leakage out (L with penalty) and total discharge (Q with penalty) as output, were generated using a calibrated groundwater simulation model. The total data is divided into three subsets: training (70%), validation (15%), and testing (15%). An FFNN with a single hidden layer and enough hidden layer size (neurons) is capable of any input-output mapping (The MathWork Inc.). But the ANN training time also increases with an increase in the size of the training dataset and layer size (neurons). This makes the combination of large training data set and layer size infeasible. Different layer sizes (20, 10, 25) were tested and the best of the ANN model was selected based on R-square and Mean Absolute Percentage Error (MAPE) of Leakage out because the total discharge predictions were accurate. Along with these matrices, the values of Maximum Absolute Error (MXAE) and Root Mean Squared Error (RMSE) are shown in Table 3.

As is evident from the table, the “Model 2”, under leakage out, is having a good R-square value (near to 0.97) and a high MAPE value (near to 25%). This means that even though the actual and predicted output are correlated, there is a significant deviation existing from the actual model. Even if the optimum points for Model 2 (ANN) are derived using evolutionary algorithms, the correct value of decision variables could not be obtained. It makes the use of this ANN model unsuitable for the optimization model for Model 2. Thus, final optimization using ANN is performed for “Model 1” and “Model 3” only.

### 3.5. Performance Metrics:

In multi-objective optimization algorithms, the solution set generated approximates the actual Pareto front. The approximated fronts are compared based on convergence, diversity, and uniformity. Various performance matrices are available that account for one, two, or all of the three aspects of the Pareto fronts. These metrics can be unary or binary. In this work, six metrics are used, namely, epsilon, spread, generalized spread, generational distance, inverted generational distance, and hypervolume (Table 4). The matrices require a reference point or reference Pareto front. The non-dominated set from the union of the points obtained from the compared Pareto front is used as the reference Pareto front and a value lower than that of the anti-utopia point of this reference front is taken as a reference point ( $1e4$ ,  $5e4$ ). A detailed comparison of various performance metrics can be found in Zitzler et. al. (2003).

The unary e-indicator metric represents the smallest distance that an approximate Pareto front must be translated to completely dominate the reference Pareto set (Kollat et. al., 2005). The average Euclidean distance between the reference Pareto set and the approximate Pareto solutions is called the Generational distance (GD). Both, epsilon and generational distance measure the convergence. The lower the value of epsilon and generational distance, the better is the convergence. The diversity of the Pareto front can be compared based on the distribution of the solution set (uniformity) and its extent. Spread and generalized spread quantifies the non-uniformity of approximate Pareto front. Small the value of these matrices indicates, a better and diverse set of approximate Pareto front. The inverted GD is the average distance between each member of the reference Pareto front and the approximate Pareto front. It is highly influenced by the distribution of the approximate Pareto front. Hypervolume measures the size of the space enclosed by the approximate Pareto front. Both, inverted generational distance and hypervolume are a unary metric that considers convergence and diversity. In addition, hypervolume is the most widely used performance metric (Riquelme et. al. 2015). Auger A. et. al. (2009) have provided a method to choose the value of reference point for the calculation of hypervolume. Unlike inverted generational distance, the higher the hypervolume better is the combined effect of convergence and diversity of the approximate Pareto front.

## 4. Results:

### 4.1 Simulation-optimization model

Each combination of the simulation model and optimization technique was evaluated up to 5000 points

depending upon the optimization algorithm and its parameters. In all the three models, the Pareto fronts by MOPSO were more converged, whereas the results obtained from GA were more diverse for model 1 and model 3 (Fig. 5). The Pareto search and MOEAD were more converged in comparison to GA, but they lack diversity. Only in model 2, the diversity of the PF of MOPSO outperforms that of GA. The solutions of GA are highly diverse in model 1 and model 3, even at a low number of simulations runs. Other than the optimization algorithm, the Pareto fronts trends are determined by the model demarcation and its boundary conditions.

To understand the impact of different model domains on optimal outputs, the best-performed MOPSO front was studied. Pareto fronts show that Domain-1 is giving a high value of leakage out in comparison of the optimal value of groundwater discharge through wells whereas the output of Domain-2 is higher than Domain-3 ex. for discharge value of 2000000 m<sup>3</sup>/day leakage out in Domain-1, Domain-2 and Domain-3 are as follows 153560 m<sup>3</sup>/day, 134940 m<sup>3</sup>/day and 100800 m<sup>3</sup>/day. The Pareto fronts (Fig. 5) also depict the effect of a model domain on the optimal discharge and river gain relation. For instance, in the case of MOPSO, an increase of discharge by 50,000 m<sup>3</sup>/day (from 200,000 m<sup>3</sup>/day to 250,000 m<sup>3</sup>/day) leads to a decrease in river gain by 15,820 m<sup>3</sup>/day, 37,657 m<sup>3</sup>/day, and 19,535 m<sup>3</sup>/day for the model domain 1, 2, and 3 respectively. Correspondingly, the Pareto search demonstrates a decrease of river gain by 22,278.9 m<sup>3</sup>/day, 40,116 m<sup>3</sup>/day, and 20,457.4 m<sup>3</sup>/day for the previously mentioned discharge increase.

All the six metrics, for the three model domains and four optimization techniques, are shown in Figure 6. The combined effect of diversity and convergence from inverted GD and hypervolume also suggests the superiority of MOPSO, in all three domains, over other optimization techniques. Further, the epsilon metric and generational distance suggest that convergence of MOPSO is best. Both the parameters, epsilon, and generational distance, show conflict in the comparison of other optimization techniques. In terms of uniformity of solutions, spread and generalized spread suggests the superiority of GA for model 1. In model 3, even though the Pareto front of GA is diverse, the solutions are not uniform due to which the spread of GA is high. For model 3, MOPSO is much more uniformly distributed and hence has a low value of the spread.

## 4.2 ANN-Optimization model

MOPSO showed significant improvement in terms of convergence, diversity, and uniformity of the solutions (Figure 7). MOEAD showed improved diversity and uniformity whereas convergence was still similar to the Pareto search (without ANN). Although GA showed no major improvement in the convergence, the uniformity of Pareto solution distribution is increased. The Pareto search solution without the use of ANN can be taken as the reference for the comparison (Fig. 5 and Fig. 7). The diversity and uniformity of the GA and MOPSO are close and comparable.

Spread and Generalized spread depict that the MOPSO and GA have a uniform distribution of the solutions. Whereas the MOEAD shows a polar and non-uniform distribution of solutions. The MOPSO is superior to other algorithms, in terms of convergence, suggested by epsilon and generational distance. The combined effect of convergence and diversity, measured with hypervolume and inverted GD, is also best for MOPSO. GA, PS, and MOEAD show a close value of hypervolume and inverted GD indicating a nearly equivalent performance in terms of convergence and diversity. The percentage increase in hypervolume and decrease in inverted GD, both show that MOPSO in model 1 and MOEAD in model 3, has significant improvement (Fig. 9). Whereas GA and MOEAD in model 1 show the least improvement. However, the GA and MOPSO (in Model 3) showed conflict in the change in values. Inverted GD is less reliable because it is strongly influenced by the distribution of the approximate Pareto front. Figure 10(a) and Figure 10(b) shows the box-whisker plot of the decision variables from the Pareto solutions obtained from each optimization technique and two (1 and 3) model domain size. It can be observed that the distribution of decision variables for the solutions is dependent on the optimization algorithm rather than the model domain size. Further, in GA the solution decision variables have a smaller number of outliers compared based on well zone distribution. A similar trend is shown in MOPSO and Pareto searches, with an increased number of outliers. MOEAD shows a broader distribution with the length of the box (25 and 75 percentiles bound) greater than other optimization techniques. MOPSO solutions have a large number of outliers depicting a large number of

solutions focused in the quartile range. The mean discharge for GA solutions is less than or close to 1000 for nearly all of the zones. In Pareto Search, the mean values are close to the bounds of the box (25 or 75 percentile) of the solutions and the mean discharge largely varies with the decision variable number (i.e., location of well zone).

Furthermore, figure 10 provides the spatial variation of the optimized well discharge. In total, there are 30 well zones in both the domains and half of them are classified as “far away” or “close” depending upon their shortest distance from the river. The average optimal discharge of faraway wells is observed to be slightly higher than those close to the river. In Model 3, the value means optimal discharge of faraway well is 860.8 m<sup>3</sup>/day and that of wells close to the river is 832.9 m<sup>3</sup>/day. However, in Model 1 the gap between the two values narrows down further, with far away well avg. discharge as 905.4 m<sup>3</sup>/day and close well avg. discharge as 901.2 m<sup>3</sup>/day.

## 5. Discussions :

The solutions of GA are highly diverse in model 1 and model 3, even at a low number of simulations runs. Other than the optimization algorithm, the Pareto fronts trends are determined by the model demarcation and its boundary conditions. It shows that adding the Rhone River in the model alters the groundwater flow correspondingly water budgeting of the area and gives the least groundwater flow into the river due to excess pumping. Results show that Model-2 which consists of the shortest area along with the dominated constant boundary inflow is providing less groundwater to the river in comparison to Domain-1 which consists of a larger area in the simulation along with a one-sided watershed boundary. It can be observed that even though all three domains extract the same amount of groundwater, the modelled effect on the river varies for each domain. In addition, the data from the Pareto front suggest that in model 2, the extraction from the well and the river gain are heavily related to each other. This relation will not only influence the simulation results but will also affect the decision-making in groundwater management. In ANN Optimization model, it is thus evident that in terms of convergence, the solution points of MOPSO dominate every other solution, and solution points of GA are dominated by most of the other points. PS and MOEAD solutions lie in between in the GA and MOPSO front for both models. MOPSO solutions largely consist of outliers with either too small or too large box bounds. MOEAD solutions are largely uniform and cover the lower and upper bound of decision variables. Regardless of the small difference, the overall trend is: wells close to rivers extract less groundwater than far away. Another factor, that can contribute to the high discharge of a close well is spatial heterogeneity in the aquifer properties.

## 5. Conclusions:

Three different domain sizes of groundwater model for optimization of withdrawal and gain in the river from the aquifer, by four different optimization algorithms were discussed. The groundwater model development, optimization models, ANN model to reduce evaluation time, performance metrics for Pareto fronts, and the comparison of the distribution of optimal decision variables for different optimization techniques, are also discussed. The ANN model for three domains shows the difference in accuracy, suggesting a change in domain size and consequently boundary conditions can alter the performance of ANN. Results show that boundary conditions and domain size influence the result of simulation-optimization models. Domain-1 was found more efficient and was capable to give a higher value of R-A exchange corresponding to the discharge of pumping wells.

The simulation-optimization model result suggests that GA provided a diverse set of Pareto solutions even for a low number of evaluations but the solution of other algorithms was dominating, with MOPSO being the best. And among the three domains, model 2 consistently implied a greater interrelation between the two costs, i.e. total discharge and river gain. In the ANN-Optimization model, MOPSO showed significant improvement in both diversity and convergence. GA solutions didn't show major improvement in convergence. This suggested the use of GA to obtain a tentative solution set that can be obtained without the use of the ANN model. The use of ANN can significantly improve the performance of MOPSO by allowing it to have a greater number of evaluations, which was limited in the raw simulation model due to the infeasible

computation time.

The distribution of optimal decision variables was well distributed for MOEAD and comparatively limited in other optimization techniques. But the distribution of decision variables didn't represent the quality of the solution from perspective of performance of optimization algorithm. In case of decision-making problems, this study can be helpful to have good distribution of decision variables, even though they provide a better solution but not the best one. Apart from statistical distribution of solutions, the spatial distribution of optimized decision variables (well discharge) provided a lot of information regarding the physical interpretation and conceptual verification of the solutions. These solutions followed an expected trend of higher discharge at faraway wells and lower discharge at the close wells. From this study, the influence of domain demarcation, boundary conditions, and optimization algorithm has been observed on the Pareto fronts and optimized decision variables. The conceptual verification of the Pareto solutions was also explained. Besides this, the use of ANN and handling the constraints of the optimization problem is also considered for a real-world groundwater problem. Still, several challenges in R-A exchange-related groundwater decision-making exist. Accurate R-A exchange modeling, precise surrogate models to reduce S-O time, and dealing with high heterogeneity of the domain, to name a few.

## References

- Dangar, Swarup & Asoka, Akarsh & Mishra, Vimal. (2021). Causes and implications of groundwater depletion in India: A review. *Journal of Hydrology*. 596. 10.1016/j.jhydrol.2021.126103.
- Anderson MP. (2005). Heat as a Ground Water Tracer. *Ground Water*, 43(6), 951-968.
- Asadzadeh, Masoud, Bryan A. Tolson, and Donald H. Burn (2014). "A new selection metric for multi-objective hydrologic model calibration." *Water Resources Research* 50, no. 9, 7082-7099.
- Atwell BH, MacDonald RB, Bartolucci LA. (1971). Thermal mapping of streams from airborne radiometric scanning. *Water Resources Bulletin*, 7(2), 228-243.
- Auger, A., Bader, J., Brockhoff, D. and Zitzler, E., (2009). Theory of the hyper volume indicator: optimal  $\mu$ -distributions and the choice of the reference point. In *Proceedings of the tenth ACM SIGEVO Workshop on Foundations of genetic algorithms*, 87-102.
- Avent, Brendan, Javier González, Tom Diethe, Andrei Paleyes, and Borja Balle (2020). "Automatic Discovery of Privacy-Utility Pareto Fronts." *Proceedings on Privacy Enhancing Technologies* 2020, no. 4, 5-23.
- Bassi, Mohamed, Eduardo Souza de Cursi, Emmanuel Pagnacco, and Rachid Ellaia (2018). "Statistics of the Pareto front in Multi-objective Optimization under Uncertainties." *Latin American Journal of Solids and Structures* 15, no. 11.
- Becker MW, Georgian T, Ambrose H, Siniscalchi J, Fredrick K. (2004). Estimating flow and flux of groundwater discharge using water temperature and velocity, *Journal of Hydrology*, 296(1-4), 221-233.
- Belakaria, Syrine, and Aryan Deshwal (2019). Max-value entropy search for multi-objective bayesian optimization. In *International Conference on Neural Information Processing Systems (NeurIPS)*.
- Binois, M., Ginsbourger, D., & Roustant, O. (2015). Quantifying uncertainty on Pareto fronts with Gaussian process conditional simulations. *European journal of operational research*, 243(2), 386-394.
- Burkholder BK, Grant GE, Haggerty R, Khangaonkar T, Wamper PJ. (2008). Influence of hyporheic flow and geomorphology on temperature of a large, gravel-bed River, Clackamas River, Oregon, USA. *Hydrological Processes*, 22, 941-953.
- Calandra, Roberto, Jan Peters, and M. P. Deisenroth (2014). Pareto front modeling for sensitivity analysis in multi-objective bayesian optimization. In *NIPS Workshop on Bayesian Optimization*, vol. 5.
- Cao, P., Fan, Z., Gao, R., & Tang, J. (2017). A manufacturing-oriented single point search hyper-heuristic scheme for multi-objective optimization. In *ASME 2017 International Design Engineering Technical Conferences and Computers and Information in Engineering Conference*. American Society of Mechanical Engineers Digital Collection.
- Coello, Carlos A. Coello, Gregorio Toscano Pulido, and M. Salazar Lechuga (2004). "Handling multiple objectives with particle swarm optimization." *IEEE Transactions on evolutionary computation* 8.3,

256-279

- Constantz J. (1998). Interaction between stream temperature, streamflow, and groundwater exchanges in alpine streams. *Water Resources Research*, 34, 1609-1615.
- Cristea NC, Burges SJ. (2009). Use of Thermal Infrared Imagery to Complement Monitoring and Modeling of Spatial Stream Temperature. *Journal of Hydrologic Engineering*, 14(10), 1080-1090.
- Deb, Kalyanmoy (2001). *Multi-Objective Optimization using Evolutionary Algorithms*, John Wiley & Sons, Ltd, Chichester, England.
- Emmerich, Michael TM, and André H. Deutz (2018). A tutorial on multiobjective optimization: fundamentals and evolutionary methods. *Natural Computing* 17, no. 3, 585-609.
- Graillet D, Paran F, Bornette G, Marmonier P, Piscart C, Cadilhac L. (2014). Coupling groundwater modeling and biological indicators for identifying river/aquifer exchanges. SpringerPlus, DOI: 10.1186/2193-1801-3-68
- Handcock RN, Gillespie AR, Cherkauer KA, Kay JE, Burges SJ, Kampf SK. (2006). Accuracy and uncertainty of thermal infrared remote sensing of stream temperatures at multiple spatial scales. *Remote Sensing of Environment*, 100, 427-440.
- Herbert C, Caissie D, Satish MG, El-Jabi N. (2011). Study of stream temperature dynamics and corresponding heat fluxes within Miramichi River catchments (New Brunswick, Canada). *Hydrological Processes*, 25, 2439-2455.
- Hernández-Lobato, Daniel, Jose Hernandez-Lobato, Amar Shah, and Ryan Adams (2016). "Predictive entropy search for multi-objective bayesian optimization." In *International Conference on Machine Learning*, pp. 1492-1501. PMLR.
- Höllermann, Britta, and Mariele Evers (2019). Coping with uncertainty in water management: Qualitative system analysis as a vehicle to visualize the plurality of practitioners' uncertainty handling routines. *Journal of environmental management*, 235, 213-223.
- Horn, D., Demircioğlu, A., Bischl, B. et al. (2018) A comparative study on large-scale kernelized support vector machines. *Adv Data Anal Classif* 12, 867–883.
- Kalbus E, Reinstorf F, Schirmer M. (2006). Estimating flow and flux of groundwater discharge using water temperature and velocity. *Hydrology and Earth System Sciences*, 10, 873-887.
- Kay JE, Kampf SK, Handcock RN, Cherkauer KA, Gillespie AR, Burges SJ. (2005). Accuracy of lake and stream temperatures estimated from thermal infrared images. *Journal of the American Water Resources Association*, 41, 1161-1175.
- Keery J, Binley A, Crook N, Smith JWN. (2007). Temporal and spatial variability of groundwater-surface water fluxes: Development and application of an analytical method using temperature time series. *Journal of Hydrology*, 336, 1-16.
- Kollat, Joshua B., and Patrick M. Reed (2005). The value of online adaptive search: a performance comparison of NSGAI,  $\epsilon$ -NSGAI, and  $\epsilon$ MOEA. *International Conference on Evolutionary Multi-Criterion Optimization*. Springer, Berlin, Heidelberg.
- Loheide SP, Gorelick SM. (2006). Quantifying stream – Aquifer Interactions through the Analysis of Remotely Sensed Thermographic Profiles and In Situ Temperature Histories. *Environmental Science and Technology*, 40(10), 3336-3341.
- Lowry CS, Walker JF, Hunt RJ, Anderson MP. (2007). Identifying spatial variability of groundwater discharge in a wetland stream using a distributed temperature sensor. *Water Resources Research*, 43, W10408.
- Marjit R. and Hopfe C.J. (2009). Multi-objective robust optimization algorithms for improving energy consumption and thermal comfort of buildings.
- MATLAB. (20\_\_). version 7.10.0 (R20\_\_a). Natick, Massachusetts: The MathWorks Inc.
- McDonald MG, Harbaugh AW. (1988). A modular three-dimensional finite-difference ground-water flow model, 6. U.S. Geological Survey Techniques of Water-Resources Investigations.
- Paran F, Arthaud F, Bornette G, Graillet D, Lalot E, Marmonier P, Novel M, Piscart C. (2012). Characterization of exchanges between Rhône River and groundwater., Research report ZABR Phase 4, AERMC

- Riquelme, Nery, Christian Von Lüken, and Benjamin Baran.(2015) Performance metrics in multi-objective optimization. Latin American Computing Conference (CLEI). IEEE.
- Salomon, Ludovic, Charles Audet, Jean Bigeon, and Sébastien Le Digabel (2018). Review of the quality of approximated Pareto fronts in multiobjective optimization, Journées de l'optimisation. In JOpt.
- Sophocleous, M. (2002) Interactions between groundwater and surface water: the state of the science, Hydrogeology Journal, 10, 52–67.
- Víctor Martínez-Cagigal (2020). Multi-Objective Particle Swarm Optimization (MOPSO) (The MathWorks Inc.), MATLAB Central File Exchange. Retrieved October 1, 2020.
- Wawrzyniak V, Piégay H, Poirel A. (2012). Longitudinal and temporal thermal patterns of the French Rhône River using Landsat ETM+ thermal infrared images. Aquatic Sciences, 74(3), 405-414.
- Wei Mao, Jinzhong Yang, Yan Zhu, Ming Ye, Jingwei Wu (2017) Loosely coupled SaltMod for simulating groundwater and salt dynamics under well-canal conjunctive irrigation in semi-arid areas, Agricultural Water Management, 192, 209-220.
- Westhoff MC, Savenije HHG, Luxemburg WMJ, Stelling GS, van de Giesen NC, Selker JS, Pfister L, Uhlenbrook S. (2007). A distributed stream temperature model using high resolution temperature observations. Hydrology and Earth System Sciences, 11, 1469-1480.
- Zhang, Qingfu, and Hui Li (2007). MOEA/D: A multiobjective evolutionary algorithm based on decomposition. IEEE Transactions on evolutionary computation 11.6, 712-731
- Zitzler, Eckart, Lothar Thiele, Marco Laumanns, Carlos M. Fonseca, and Viviane Grunert Da Fonseca. Performance assessment of multiobjective optimizers: An analysis and review. IEEE Transactions on evolutionary computation 7, no. 2 (2003): 117-132.

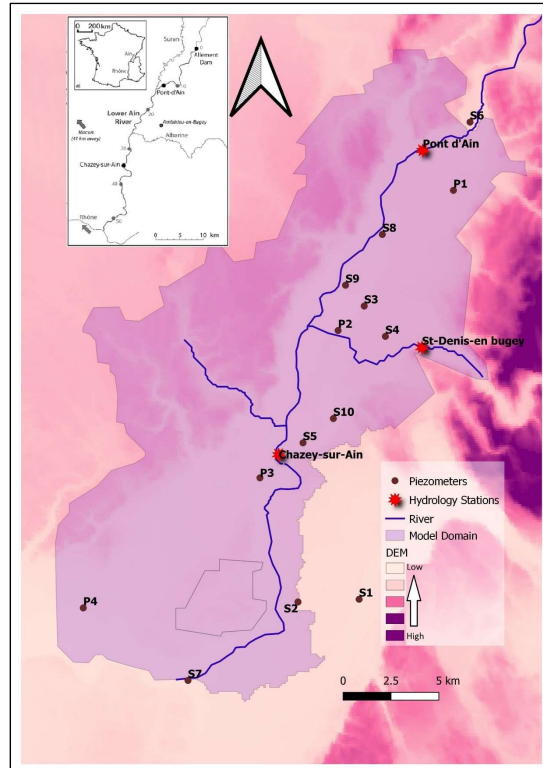
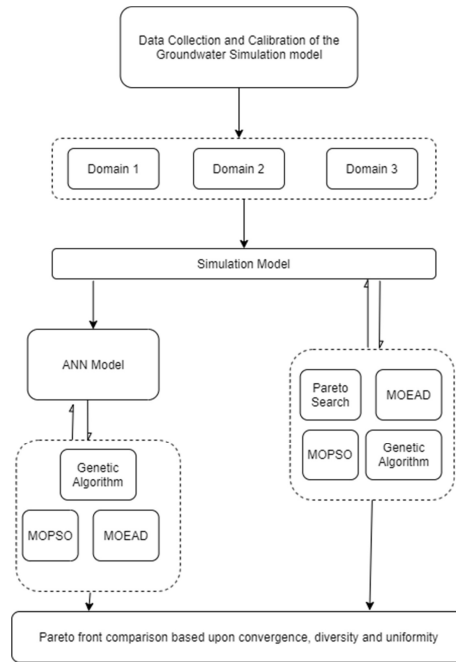


Fig 1: Study Area



**Fig 2: Flow chart showing the 2 main steps in the optimization process considering (1) different in boundary conditions and (2) with and without speeding up calculation using ANN model**

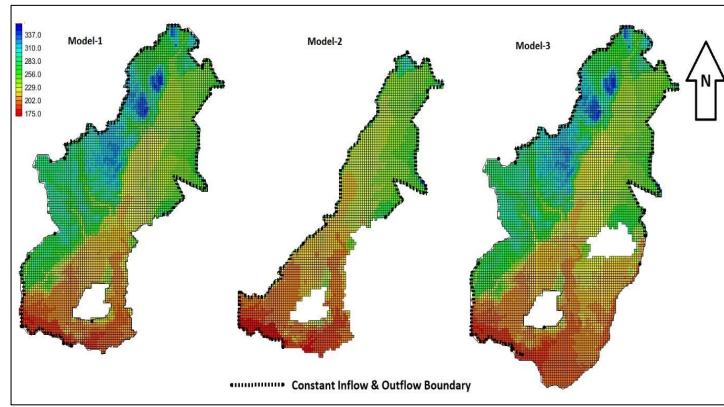


Fig 3: Different Groundwater Modelling Domains

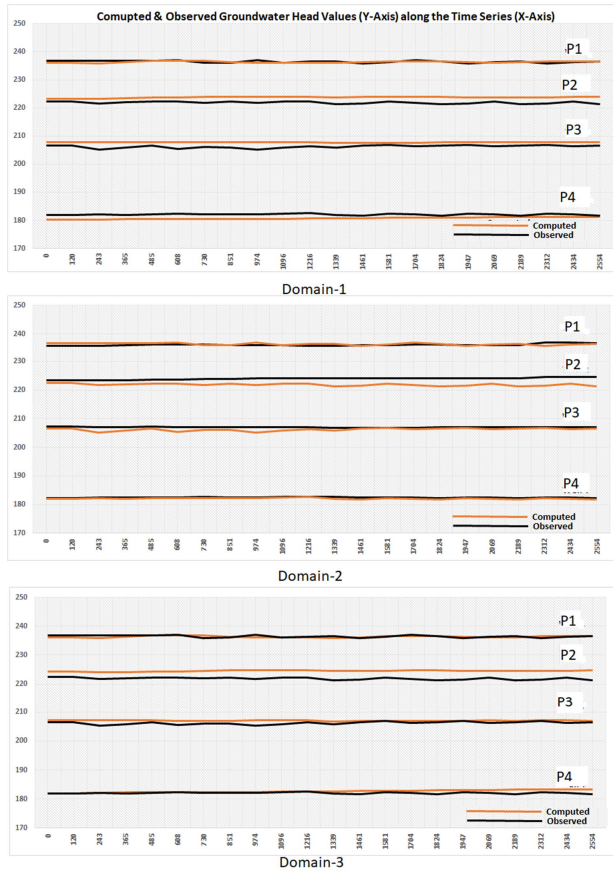
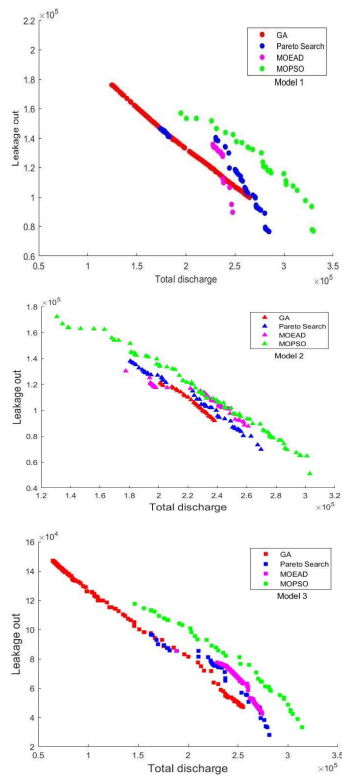
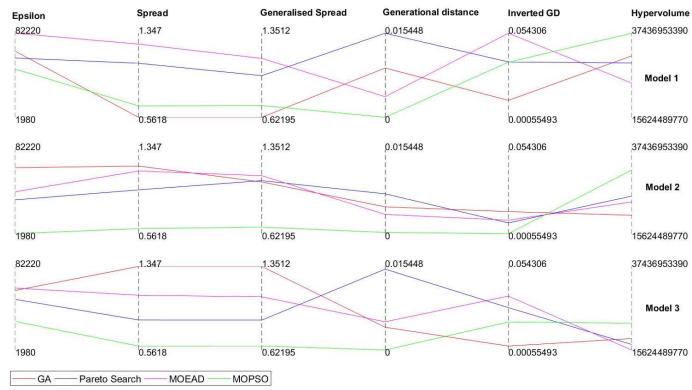


Figure 4: Calibration graph for each model domain (see Figure-1 for locations).



**Fig. 5 Pareto front comparison of optimization techniques through Simulation-Optimization model**



**Fig. 6 Metrics for the comparison of optimization techniques for a smaller number of evaluations**

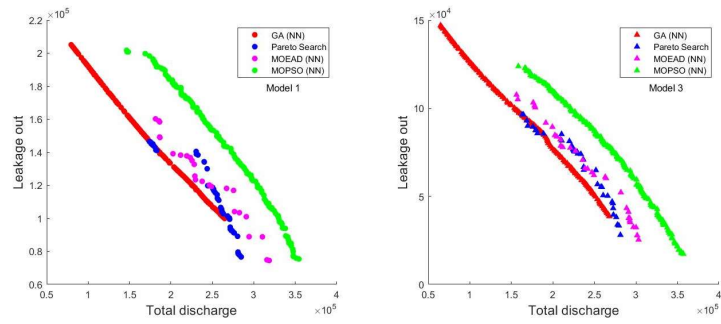


Fig. 7 Pareto front comparison of optimization techniques with ANN models

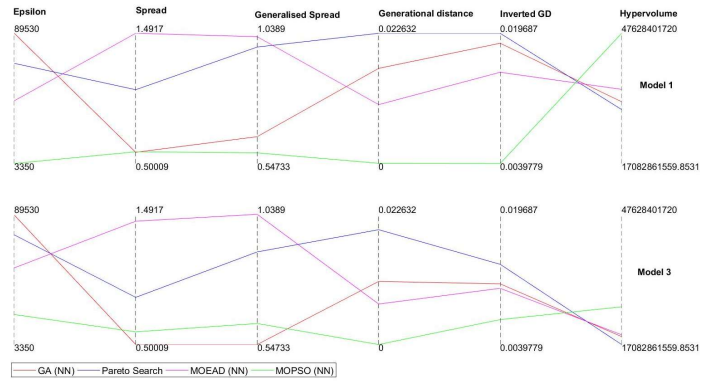
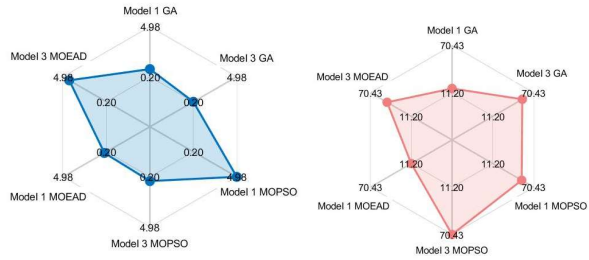
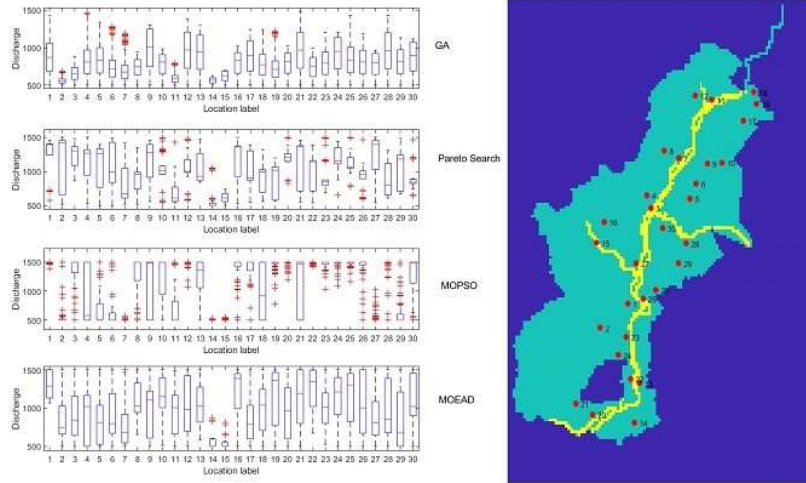


Fig. 8 Metrics for the comparison of optimization techniques with ANN models



**Fig. 9 Percentage (a) increase in hypervolume (b) decrease in IGD, after introduction of ANN**



**Fig 10 (a) box whisker plot of zone wise optimal discharge of different optimization algorithms for Model 1**

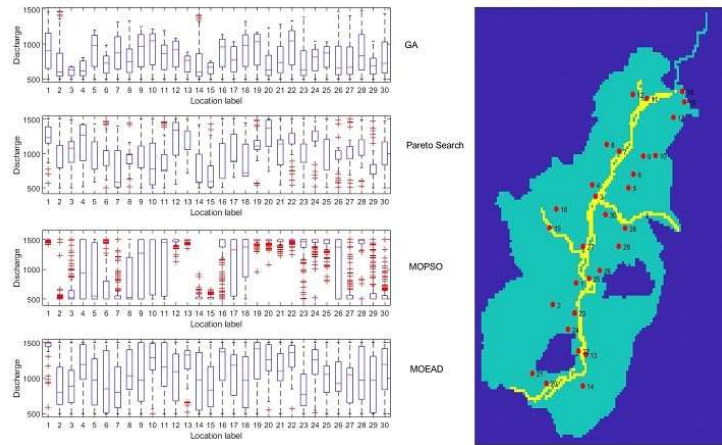


**Fig. 10 (b) box whisker plot of zone wise optimal discharge of different optimization algorithms for Model 3**

### Hosted file

Tables.docx available at <https://authorea.com/users/435384/articles/538448-optimization-of-groundwater-pumping-and-river-aquifer-exchanges-for-management-of-water-resources>